Analyzing Dark Matter and Its Indirect Detection

Daniel Martinez and Rohith Sajith

August 3, 2018

Contents

1 Abstract

In this paper, we strive to develop qualitative and elementary-quantitative understandings of the fundamental nature of dark matter (DM) and indirect searches for it. On the macroscopic scale, we elucidate the astronomical observations throughout the past century that have directly pointed towards of this-so-called "dark gravity," such as rotation curves, gravitational lensing, and DM density distributions. We present plots from N-body and hydrodynamic simulations that further reinforce how DM possesses great gravitational influence in the formation of galaxies and clusters. On the particulate level, we describe current research in that attempts to pin down the WIMP (Weakly Interacting Massive Particle) as the fundamental particle that comprises DM. In outlining the cosmological history of DM and its interactions with baryonic matter, we uncover greater understanding of DM indirect detection and utilize the processes of WIMP annihilation and decay to propose further avenues of research. Finally, we conclude by summarizing results in direct detection, as well as other theories that aim to conceptualize observations associated with DM.

2 Introduction

To physicists in the 1900s, the entire universe was what could be seen with the naked eye. They conjectured that the vast spaces in between stars and other astronomical objects merely consisted of an utterly empty vacuum and were confident that all matter in the universe interacted with some form of electromagnetic radiation, thus constituting it visible matter.

After Einstein's revolutionary papers of 1905 and his theories of general and special relativity, the idea of space was put into question once again, causing physicists to doubt whether universe was more than what light could uncover. From these qualms, the first evidence of *dark matter* (DM) emerged. [1]

These astrophysical phenomena included the observed velocities of stars in galaxies other than the Milky Way, as well as gravitational lensing that conflicted with data implied by Einstein's general theory of relativity. [2] It was evident that there were peculiar gravitational effects being provoked by non-visible entities. [2] After physicists conjectured DM, it seemed to explain many of the anomalies decently well, but gaping holes still existed in the understanding its origin and underlying particulate makeup. Ultimately, this paper details the astronomical and particle nature of DM, and we will review past and current efforts in indirect detection of DM.

We first prove the existence of DM by examining three staple phenomena explained by DM and its interactions with baryonic matter. Once we review this, we observe DM halos and density distributions among various galaxies. In particular, we inspect the various profiles of DM density (throughout the paper) and utilize N-body simulations to model the gravitational effects of DM and baryonic matter. Finally, we review current DM searches for useful quantities (cross sections, J-factors, emissions), develop a common framework for contemporary DM indirect detection through annihilation processes, and discuss methods to refine current procedures on detection. [3]

To conclude, we provide a brief description of other theories for DM that were not already discussed. We explain how the axion, which was created to solve a polarity problem within water molecules, can be a candidate for DM itself. Finally, we study direct detection, another field where much DM detection research exists, and how its findings complement ours.

3 Proof of Dark Matter Existence

3.1 Rotation Curves

Evidence for DM began to quickly emerge in the 1900s from astrophysicists. [4] However, while the underlying makeup of DM was not definitive, it was apparent that DM possessed mass; thus, the bulk of support for DM came from gravitational properties. [1] Using solely Newtonian Mechanics within a Galactic system, we can easily derive velocities of stars orbiting the center of the Galaxy:

$$a_c = \frac{v^2}{R} = \frac{GM}{R^2} \to v = \sqrt{\frac{GM}{R}},$$

where R is the orbital radius of the star in question and M is the mass of the *visible* matter enclosed inside the star's orbit. [1] From this simple model, it becomes clear that as we increase our distance from the center of a galaxy that - since M is roughly constant - that $v \propto R^{-0.5}$.

Despite this, what is actually observed through a plethora of galactic evidence is that stars at the perimeter of galaxies move significantly faster Newtonian physics predicts - as R increases, $v(r)$ stays roughly constant instead. [2]

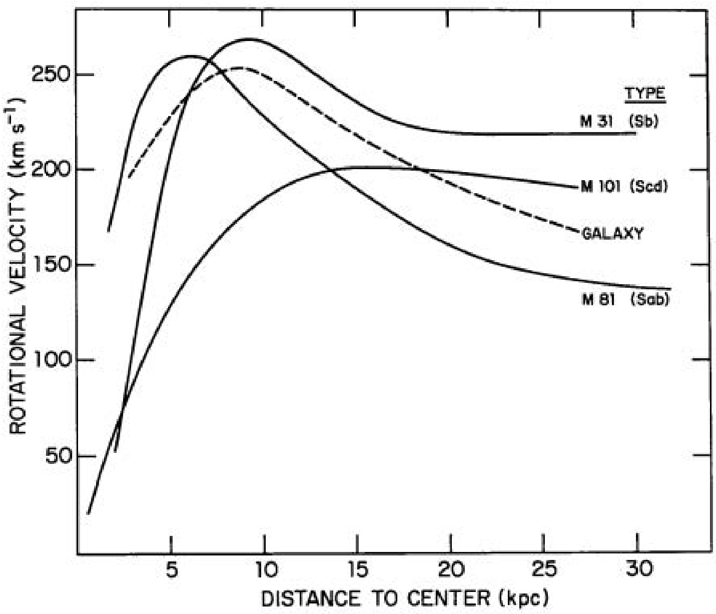

Figure 1: Vera Rubin and Kent Ford recorded the above rotation curves for various galaxies and saw a general result - while Newton had predicted that velocities would slope down at R^{-2}, the curves were staying roughly constant instead. [31] Figure from [23].

These rotational curves, as shown in Figure 1, provided arguably the strongest evidence of additional mass within galaxies that was at the time invisible and undetectable. [4] The existence of this mass was further seconded by Lord Kelvin and Henri Poincaré, both of whom found a discrepancy between the amount of matter dictated by observation and that based on the mere velocities of the bodies. Poincaré, in order to explain this phenomena, coined the term "dark matter," attempting to describe a form of gravity that was not indicative of luminous matter. In reality, we are not certain whether DM is even a form of matter, but the majority of contemporary research is devoted to confirming this theory. [5]

The observed rotational curves imply that as R increases that $M(R) \sim R$, meaning that the mass density of this DM is roughly

$$\rho(r) \propto \frac{M(R)}{R^3} \propto \frac{1}{R^2}.$$

It is important to note that the volume term above has been assumed to be a sphere based on the following premise: Baryonic matter, due to the conservation of angular momentum universe, radiates off energy due to energy-induced gas. However, the loss of energy from this gas will cause the ratio of angular momentum to total energy $\frac{L}{E}$ to increase, causing a disk-like shape. [4] DM as we know it today, however, does not possess such radiative properties that motivate the formation of a disk and is thus postulated to exist freely in the shape of a sphere. [5]

The above estimate provides a very crude approximation for the density distribution of DM, which will be made more precise in later sections.

3.2 CMB

While much of the direct data regarding DM can be quite imprecise, the acoustic fluctuations of the universe at the time of recombination in the Cosmic Microwave Background Radiation (CMB) have measurements that are fairly conclusive - this enables physicists to both infer the existence of DM and extrapolate its properties. [4] (the latter will be discussed in later sections.)

Due to the small quantum density anisotropies in the early universe, matter, due to gravitational interaction, began to cluster in areas of greater density and higher gravitational potential, causing even larger anisotropies. [6] Before the recombination event at $t = 378,000$ years, baryonic matter, in the form of protons, electrons, and photons, was in a state of plasma, characterized by extremely high energy states. [6] As a result, when such an excited plasma began to fall into gravitational wells, the photons, due to their extremely high abundance, began to fall in between protons and electrons and acted as an elastic pressure force - as photons were compressed past their "equilibrium states" within an anisotropy, they started to decompress, ultimately counteracting the force of gravity. Thus, the "back-and-forth" motion of gravitational pressure and photon decompression caused oscillations in the fabric of space itself - the oscillations were not unlike a harmonic oscillator. [7]

By breaking down the density fluctuations as the sum of many simpler wave functions through Fourier Analysis, we are able to see the different components of the universe's early wavering motion at varying angular frequencies and wavelengths. At recombination, when photons had escaped from between protons and electrons, the oscillations stopped, and what we observe as the CMB is the "fingerprint" of the oscillation at $t = 378,000$ years. (After this time, the photons were allowed to roam free and no longer scattered off protons and electrons frequently, so this is referred to as the "last scattering.") The density fluctuations of the CMB in the fabric of space are what gravitationally allow galaxies and solar systems to settle down and form. [7]

Graphing the fluctuations mentioned above as a function of angular frequency yields the following curve:

The peaks of the graph indicate the instant when a relatively large amount of matter had clustered inside a well, but the decompression force had not yet taken effect; this lack of baryonic pressure causes a peak in fluctuation.

A trough, on the other hand, dictates when the photons have reached their maximal "elasticity" and have stretched out of the anisotropy as much as possible. [6]

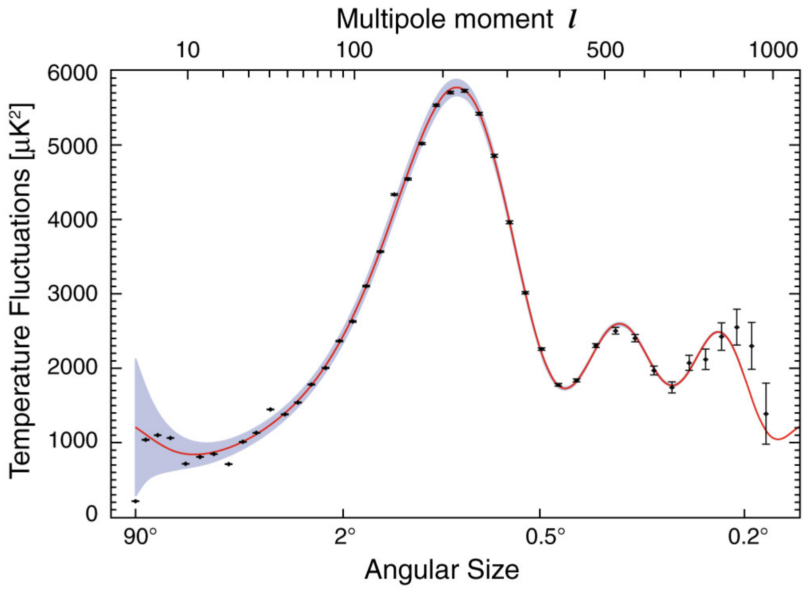

Figure 2: Through decomposed wave functions, we observe different peaks of density corresponding to the landscape of the universe at the time of recombination. These baryonic acoustic oscillations ultimately shed light on what wave frequencies (and thus density levels) were most prevalent at $t = 378,000$. Figure from [27].

The relative magnitudes of the first peak and trough indicates an interesting fact: if there were only baryonic matter in the universe, then the counteracting pressure force would be approximately equal in strength to the gravity of the anisotropies, which would imply equal magnitudes within the graph. [7] However, it is clear that the peak is significantly larger, suggesting that the influence of gravity within wells is greater than the photons' counteracting force. Thus, scientists can infer that there must exist a form of "matter" within the anisotropies that interacts only through gravity and does not possess baryonic elasticity, as observed in the CMB. This not only demonstrates the existence of DM, but also that it is approximately five times larger in energy density as baryonic matter ($\Omega_{\rm DM} = 0.22, \Omega_{\rm BM} = 0.04$.) [7]

The significance of the CMB will become more apparent in bounding certain quantities later.

3.3 Gravitational Lensing

Due Einstein's Theory of General Relativity, space and time were theorized as being conjoined into a single fabric, and gravity, the very familiar force, began to be interpreted as the curvature of this fabric.

As evidenced by views of eclipses, the curvature of spacetime bends light around areas of relatively high gravitational potential, such as our Sun, large galaxies, or black holes. [9] Often after computing the rotation curves of galaxies as shown above and their corresponding masses, we observe the images of other astronomical objects behind this galaxy is significantly more smeared and lensed than we predict - this once again suggests that there must be some not luminous matter within galaxies that is motivating this extremely large gravitational influence. [9]

The distortion caused by gravitational lensing is condensed into the equation

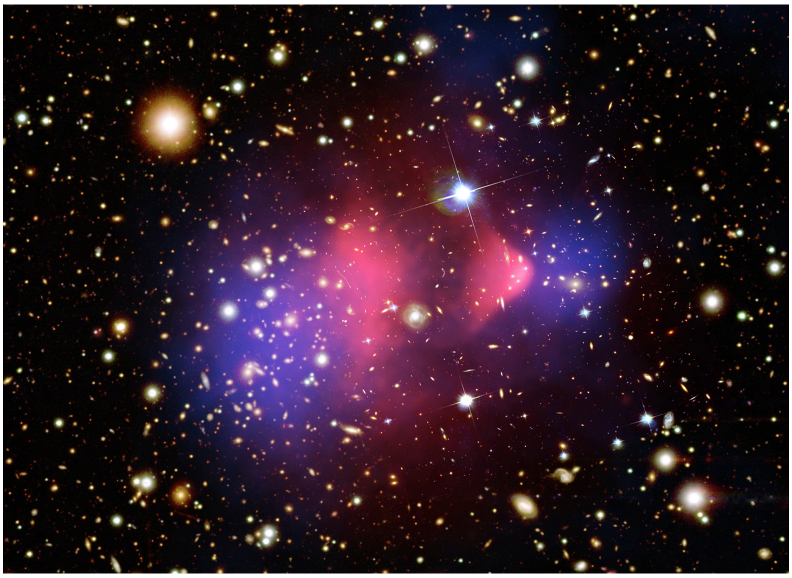

Figure 3: The red area depicts the baryonic core of the cluster, while the blue exterior portions denote the postulated DM halo that extends beyond the core of the cluster. After significant testing, physicists obtained a P-value of 10^{-15} rejecting the claim that there was not a segregation between DM and baryonic matter. The cluster's importance towards DM manifests itself in that such a convincing P-value has not been collected from any other observation. [32] Figure from [24].

$$\vec{\theta}_S = \vec{\theta}_I - \frac{D_{LS}}{D_{OS}}\vec{\alpha}(D_{OL}\vec{\theta}_I),$$

where $\vec{\theta}_S, \vec{\theta}_I$ indicate the actual and observed positions of the source, D_{LS}, D_{OS}, D_{OL} indicate respective distances from the gravitational lens, observer, and the source, and α is a function that embodies the gravitational potential of the source. [8]

After initial observations which led to the discovery of Dark Matter, the specific paths of light crossing near galaxies and clusters in weak and strong gravitational lensing respectively lend useful insights on how DM is distributed within galaxies. The feats to be conquered here are correctly mapping out the dark matter even as it is sheared by the gravitational lens and filtering out any external gravitational potential or elliptic data that could confound the data. [8]

Overall, lensing will potentially enable physicists to map out the landscape of DM within the universe, arguably the most crucial problem in DM physics. Inverting the DM mass map utilizes both local and global techniques and further dividing up DM energies into their rotational and gradient parts. The filtering process consists of methods proposed by Bayesian Methods and Gauss, both attempting to exact signals and reduce interference from other gravitational sources that would cause error. [8]

The Bullet Cluster, as shown in Figure 3, served as a prime location for DM evidence in 2006. The light from several of the galaxies behind the Bullet Cluster had been significantly lensed. Because the background images had been so significantly distorted, its discovery seconded the existence of DM and proved DM extended far beyond the baryonic core of the cluster. [32]

4 Dark Matter Distributions

4.1 Halos

In this section, we explain how DM is distributed in a spherical halo around a galaxy and within a cluster. Since DM makes up 85 percent of the matter in the universe, a comprehension of its distribution is invaluable before we can move further with its detection. [1] To reiterate from above, unlike baryonic matter which tends to form disks due to mutual collisions canceling each other out and dissipating energy, DM coalesces into spherical halos due to its higher energy compared to baryonic matter.

The roughest estimation for the mass density of DM is the isothermal sphere potential and comes from our analysis of rotational curves

$$\rho(r) \sim \frac{1}{R^2}$$

since $M(R) \sim R$. This equation assumes that the rotation curves we observed are flat; this was cleared up through N-body and hydrodynamic simulations with DM only throughout the 1990s where more precise profiles later emerged.

To provide the reader increased intuition on the scales of halos, we utilize a simple Newtonian computation - it helps us comprehend exactly what proportion of the matter in galaxies, clusters, and ultimately the larger universe is composed of DM. To find the radius of the DM halo, we operate with the constants $M_{\text{halo}} \sim 10^{12}\ M_{\odot}$ and $\rho_0 \sim 0.3\ \frac{\text{GeV}}{\text{cm}^3}$:

$$M_{\text{halo}} = 4\pi \int_0^{R_{\text{halo}}} \mathrm{d}\mathrm{r}\,\mathrm{r}^2\,\rho(r) \longrightarrow R_{\text{halo}} \sim 100\ \text{kpc}$$

where $\rho(r)$ is assumed to be radial power law function of order -2. [2] With this knowledge, we can understand how DM is not only distributed in galaxies, but also in the universe. This equation can also be applied to large galaxy clusters to receive a rough approximation of the combined extent of DM in various galaxies. [4]

DM densities in the halos will help with our grasp of the annihilation process later in this paper since areas of high DM density will be more likely to collide and annihilate to from influxes of Standard Model (SM) particles that can be detected.

4.2 DM Density Profiles

Through extensive study of N-body and hydrodynamic simulations, physicists have attempted to conform their analytical models with both the results of simulations, as well as observational data. [10]

In 1995, Julio F. Navarro, Carlos S. Frenk and Simon D.M. White ran numerous DM-only N-body simulations to model the density of DM. [5] These simulations measured the density fall off of our galaxy and gave way to the equation that is used by most commonly by physicists today:

$$\rho_{\text{NFW}}(r) = \frac{\rho_0}{\frac{r}{r_s}\left(1 + \frac{r}{r_s}\right)^2}.$$

[30] We notice that as $r \ll r_s$ the density will be proportional to $\frac{1}{r}$; on the other hand, if $r \gg r_s$, the density will fall off at $\frac{1}{r^3}$. [4] This double power-law structure is indicative of many DM density profiles - the NFW generalized profile extends this structure:

$$\rho_{\mathrm{GNFW}}(r) = \frac{\rho_0}{\left(\frac{r}{r_s}\right)^{3-\alpha}\left(1+\frac{r}{r_s}\right)^{\alpha}},$$

where $0 < \alpha < 3$ is a constant that dictates steepness. [11] Searches and simulations by Fukushige have placed bounds on β to $0.8 < \alpha < 1.5$ [11]

Note that these DM density profiles apply not only to single galaxies, but also Galaxy Clusters. From current knowledge of N-body simulations, the NFW profile provides a largely encompassing model of DM only N-body simulations; however, certain higher resolution simulations utilize the Einsato Profile:

$$\rho_{\mathrm{Einsato}}(r) = \rho_0 \exp\left[-\frac{2}{\gamma}\left(\left(\frac{r}{r_s}\right)^{\gamma} - 1\right)\right],$$

where r_s and γ are constants for given galactic systems. The profile conforms roughly to the original NFW, but at intermediate radii, it possesses a more shallow slope, as opposed to the steep power law. [1]

Both the Einsato and the NFW profiles, however, do not take into account that the plethora of observational evidence that the density distributions have "cores," or flat interior regions. [12] This is likely due to the fact that Einsato and NFW were derived in DM only N-body models - the development of better simulations (through projects like Illustris at MIT and FIRE at Caltech) including baryonic matter could potentially improve these profiles. [12] Below are the logarithmic plots of several DM density profiles:

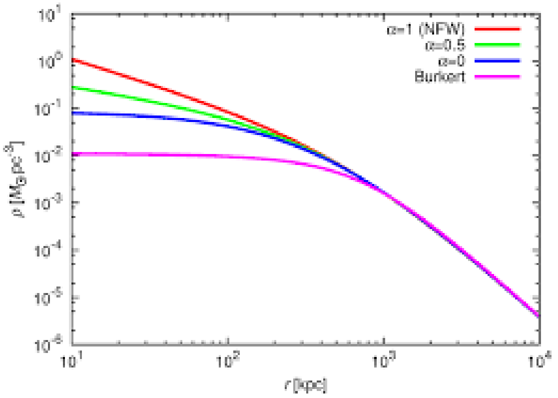

Figure 4: Different density depictions of the DM halo in the Milky Way extending from the Galactic Center (NFW, GNFW, and Burkert (to be discussed later)). Figure from [28].

It is also crucial to see how DM distributions impact the overall disk shape structure and stability of the overall galaxy. The Q factor

$$Q = \frac{c_s \kappa}{\pi G \Sigma},$$

where c_s is the speed of sound, κ is the epicyclic frequency, and Σ is the surface density of the disk, indicates that a galaxy is stable if it is greater than 1 (not undergoing star formation). [13] In general with a fairly symmetric halo, the DM serves to increase the value of Q, preventing the formation of instabilities or bars. However, if the halo is not symmetric, the κ value is altered, so the DM can acquire a certain fraction of the baryonic matter's angular momentum, which can perpetuate bar formation. [13] In most cases though, the DM's friction with most of the other baryonic matter causes much angular momentum transfer that eliminates bars. N-body simulations have confirmed that without DM within the central bar area of a galaxy that a flux of angular momentum, instead of being transferred to the DM, gets transferred from in and out of the disks, ultimately weakening any instabilities, but to a lesser extent than the DM. [13]

4.3 Cusp vs Core Density Problem

In the larger landscape of DM density distribution refinement, an essential issue to be resolved is the core-vs-cusp problem. Currently, the highest resolution N-body simulations dealing with solely DM, and not baryonic matter, produce steep power-law functions that decrease very quickly as the distance from the center of a galaxy or cluster increases - this is referred to as a cusp. [12] On the other hand, when exploring the actual galaxies, we observe that towards the centers of galaxies the cusps flatten out significantly, which referred to as cores. The problem resides in discovering how baryons interact with the DM (we discuss this more in detail in a later section). [12] Profiles such as the Burkert, which takes a very mathematical structure as the NFW, assumes a constant inner core and takes the form

$$\rho_{\text{Burkert}}(r) = \frac{\rho_s}{\left(1 + \frac{r}{r_s}\right)\left(1 + \frac{r}{r_s}\right)^2}.[1]$$

While the Burkert profile somewhat conforms to observational data, it does not shed light onto exactly why cores form.

Due to this uncertainty in the DM density profiles, observational data is limited in computing annihilation rates, cross sections, and other useful quantities within 2 kpc of the galactic center, leading to potential uncertainties in detection signals. [12] In essence, solving the Cuspy Halo Problem is essential in not only understanding the structure of the galaxy, but also whether the WIMP helps indirect detection.

5 Indirect Detection

5.1 Introduction

This section builds off previous sections to present a view on particle indirect detection of DM. We will dive extensively into the Weakly Interacting Massive Particle (WIMP), which is the most accepted model for the particulate form of DM. Then, we will present and shortly derive equations that model DM annihilation detection from gamma ray and neutrino emission signals - here we will also outline important locations for DM detection, such as the Galactic Center and Dwarf Galaxies and their significance. [1] Finally, we will discuss the predicted DM decay to occur in the future.

5.2 WIMPS

In search for potential candidates for DM, scientists had several criteria to check to ensure conformation with the experimental phenomena. The particle needed to have a lifetime constant τ that was larger than that of the observable universe (to be discussed in decay), it needed a relic density

$$\Omega_X = 0.22$$

in accordance to galactic rotation curves, and it needed to be electrically neutral. [5] Certain SM particles like neutrinos and other astronomical phenomena such as primordial black holes fit these criteria, so physicists began to look at particle cross sections to further discern particles within their searches.

After a certain amount of time following the last scattering, it can be assumed that the relative abundance of DM particles began to freeze-out - that is, the rate at which particles were created was equivalent to the expansion rate a of the universe:

$$\frac{n_c}{\langle \sigma v \rangle} < H$$

(H denotes a hubble time and n_c is the number density of the WIMPS.) Moreover, we can describe the rate at which n decreases as a function of time as

$$\frac{\mathrm{dn}}{\mathrm{dt}} = -3Hn - \langle \sigma v \rangle [n^2 - n_{\mathrm{eq}}^2],$$

where n_{eq} indicates the equilibrium number density. [14]

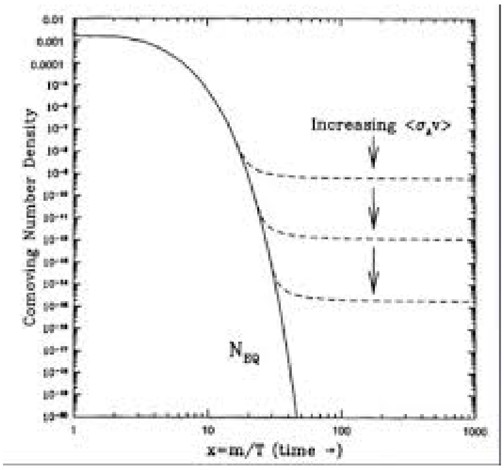

Figure 5: This plot depicts the various freeze-out densities in accordance to different values of $\langle \sigma v \rangle$, as predicted by the relative abundance differential equation above. Figure from [35].

In order to maintain the "freeze-out" density of DM (approximately five times the density of baryonic matter), a certain velocity-averaged annihilation cross section (WIMP and anti-WIMP pairs colliding) is necessary, being

$$\langle \sigma v \rangle = 3 \times 10^{-26} \, \frac{\mathrm{cm}^3}{\mathrm{s}} \sim 10^{-10} \text{ GeV}.$$

[14] This cross section miraculously is nearly identical to the cross section of particles that interact via the weak nuclear force with an energy of about 100 GeV - as a result, scientists now possessed deep motivation to deem the DM particle the "Weakly Interacting Massive Particle," as a result of this WIMP Miracle. [4]

Without concrete evidence for the WIMP through either direct or indirect detection, not many more conclusions could be made. We now discuss in detail the structures utilized in DM indirect detection.

5.3 A General Framework for Particle DM Indirect Detection for Annihilation

Indirect Detection hinges on the annihilation of DM particles - if there exists some particle annihilation process of DM that ultimately yields SM particles at the end of reaction, then there is potential to detect such particles and back trace them to obtain DM properties. [14] In an ideal sense, this is a perfect way to indirectly detect DM WIMPs - however, many astronomical phenomena (black holes, quasars, supernovae) often cloud the detection sites with additional SM particles, causing a distinctive spike in the abundance to fade. [14] We now present the common framework by which detecting a spike is possible.

Let us assume the simplest of cases - Two WIMPs self-annihilate to produce two arbitrary SM particles ξ:

$$\chi\chi \to \xi\xi.$$

First, we must compute the annihilation rate of a single particle, after which we can scale the measurements to all particles within a particular distance and solid angle. By definition, this is simply equivalent to the number density of the DM WIMPs multiplied by the annihilation cross-section:

$$\text{Single Annihilation Rate} = \frac{\rho(\mathrm{r}, \mathrm{l}, \psi)}{\mathrm{m}_\chi} \langle \sigma \mathrm{v} \rangle_{\chi\chi \to \xi\xi},$$

where r is the radial distance of the annihilation site from the center of the galaxy, l is the line of sight distance from the Earth to the annihilation site, and ψ is the angle contained by the line of sight and the radius from the Earth to the center of the galaxy. [2] These parameters may by inserted into the NFW profile to compute the DM density at the location in question.

However, this rate being for a single particle, we must scale up the rate with regard to all of the particles inside the galaxy, which can be done by multiplying the above rate by the number density and a given volume (ultimately, the number of DM particles):

$$\text{Total Annihilation Rate} = \text{Single Annihilation Rate} \cdot \text{Number Density} \cdot \text{Volume} = \frac{\rho^2}{2m_\chi^2} \cdot \langle \sigma v \rangle \cdot dV$$

(Note here that we must divide by 2 since each annihilation has two DM particles). [2] However, to get meaningful data from this formulation, we should see a spike, or a flux increase, in the number of events N of SM particles detected. Based on what SM channel ξ we choose (gamma ray, neutrino, W, Z, quark etc.), we detect events through different processes (to be discussed later). Regardless, this flux must be integrated throughout the whole solid cone between the site of interest and the earth.

By simple geometry, we can express a small volume unit dV of the cone of interest as a function of the line of line of sight distance and the solid angle measured at:

$$dV = l^2 dl d\Omega.$$

As a result, we can integrate over l and Ω to get the total flux Φ of particles for a particular energy, which is:

$$\frac{d\Phi}{dE} = \frac{1}{4\pi} \int d\Omega \underbrace{\int \frac{\rho^2}{2m_\chi^2} dl}_{\text{Astrophysical}} \underbrace{\langle \sigma v \rangle \frac{dN}{dE_\chi}}_{\text{Particle}} .[10]$$

5.4 Analysis of Equation and Implications

We explain the equation's particle component followed by its astrophysical features.

We now clarify what N signifies. For gamma ray detection (when one of the ξ is γ), N indicates the number of gamma ray annihilation events with the DM (The other ξ particle can be W boson, Z boson, quark, antiquark, or another γ). [2]

On the other hand, if $\xi = \nu$ and we are dealing with neutrino annihilation, then we are required to utilize electron scattering to detect the neutrinos at experiments such as the Super-Kaniokandr in addition to the $\chi\chi \to \nu\nu$ process. The number of events N in the neutrino reaction is

$$N = \Phi_{\mathrm{GC}} T \sigma_{\nu \to e^-} N_{e^-},$$

where Φ_{GC} is the flux of neutrinos from the galactic center observed by our detector, T is the duration of the experiment, $\sigma_{\nu \to e^-}$ is the cross section of neutrinos colliding with electrons, and N_{e^-} is the number of electrons in our detection system. Thus, though neutrinos are not directly observable, the technique of neutrino DM indirect detection can be achieved by observing the energy of excited electrons. If physicists are able to capture a distinctive "spike" in electron energy above the multitude of background sources, then this will provide strong evidence of WIMPs annihilating. [5]

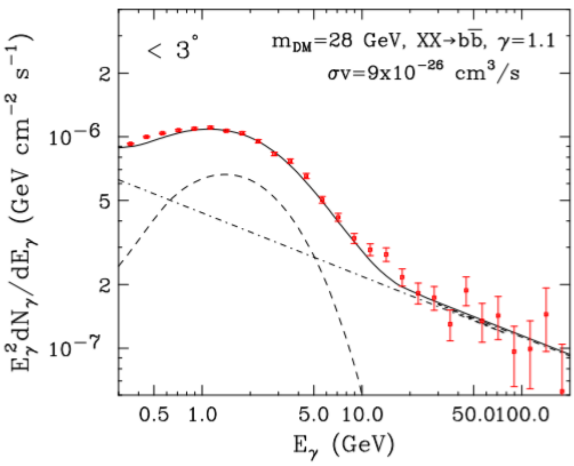

Figure 6: The graph depicts the Gamma Ray flux from both astronomical interference, the predicted flux from NFW profile, and the sum of the results. This is referred to as the Galactic Center Excess (GCE) Figure from [22]

The challenge comes in taking into account all of the background radiation caused by star light, quasars, and, most importantly, atmospheric neutrinos. Until the external sources of gamma rays are definitely pinned down, the existence of WIMPs cannot be substantiated.

Now, we discuss J-factors, which essentially embody how fruitful a search for DM is within a given area. The J-factor for DM annihilation is

$$J = \int\int \rho^2(l, \Omega) dl d\Omega,$$

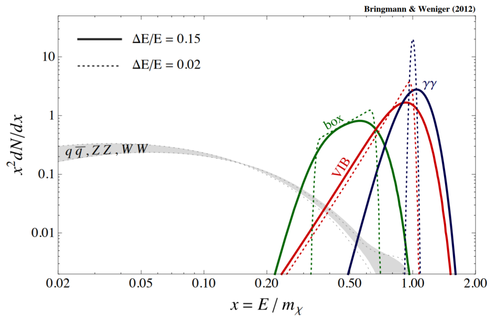

Figure 7: Different SM particles, after many annihilation processes, exist at different energy levels and produce varying fluxes and number of events over energies. Photons, in general, yield relatively distinct spikes of energy across both annihilation proceses (Blue and Red) and decay processes (Green), while quarks and W and Z bosons (Gray) create a more nuanced curve. Consequently, the former is a more fruitful candidate for detection than the latter. Figure from [21].

which, being nearly identical to the first part of the flux equation, computes a convenient abundance for the number of DM particles as it is integrated along the line of sight and throughout a larger solid cone. [15]

The difficulty of this integral is that we must integrate along the line of sight - often not tangential or radial to the source of DM - so the rate at which the DM density changes must be computed through projecting the line of sight onto the radius. As a result, we introduce additional formulas that allow us to compute J-factors in a more straight forward manner. If we utilize the simple double power law NFW profile presented above, the J-factor, after manipulation, is

$$J = \frac{25}{8G^2}\frac{\sigma^2\theta}{DR_h^2},$$

where R_h is the half-light radius of stars, D is the decay factor, σ is the luminous squared velocity distribution, and θ is the angle of integration. [15] More generalized versions of the NFW profiles and also other density profiles possess other simplifications here. The above expression also necessitates that there is a cusp in the DM density distribution. (This formula is used mostly for dwarf galaxy locations).

We present the approximate J-factors for different sources utilizing the NFW profile [15]

Name	Distance[kpc]	$\theta_{\max}$	$\log_{10} J(\theta_{\max})[\mathrm{GeV}^2\mathrm{cm}^{-5}]$	$\log_{10} J(0.5°)[\mathrm{GeV}^2\mathrm{cm}^{-5}]$
Sextans	86 ± 4	1.7	$18.04^{+0.29}_{-0.29}$	$17.87^{+0.29}_{-0.29}$
Ursa Major	76 ± 3	1.37	$19.18^{+0.24}_{-0.24}$	$19.15^{+0.25}_{-0.24}$
Boötes	66 ± 2	0.47	$16.64^{+0.64}_{-0.38}$	$16.65^{+0.64}_{-0.38}$
Reticulum II	30 ± 3	1.0	$18.72^{+0.85}_{-0.32}$	$18.71^{+0.84}_{-0.32}$

Clearly, a higher J-factor increases the chances of observing a spike in energy - still, we must take into account the amount of interference from other sources of gamma-rays, or neutrinos. Dwarf galaxies, as a result, despite lower J-factors thus are still great candidates for DM annihilation detection. Since dwarf galaxies hold relatively low amounts of baryonic matter and high amounts of DM, we can use them as great sources for DM indirect detection. The Galactic Center, for its particularly large J-factor of approximately 10^{22}, is also a fruitful location.

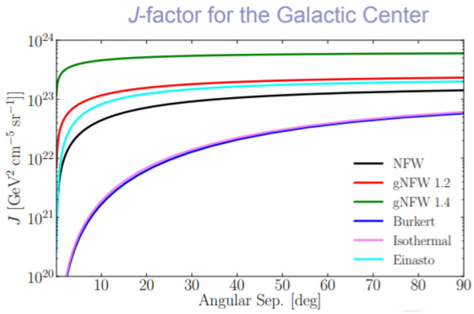

Figure 8: Additional J-factors for the Galactic Center from different DM Density profiles. Figure from [29]

5.5 CMB Revisited

As discussed before, the small anisotropies in the early universe were what caused the Cosmic Microwave Background (CMB). The DM annihilation and decay within the early universe inserted additional energy into the sea of protons and electrons - this ionized electrons from their respective hydrogen atoms, thus altering the anisotropies. However, notice that all energy ejections from the dark matter annihilations are not necessarily entirely directed towards modifying the time of hydrogen ionization. The rate at which energy is being ejected purely from annihilation can be expressed as

$$\frac{dE}{dV\,dt} = (1+z)^6(\rho_c)^2\frac{\langle\sigma v\rangle}{m_\chi},$$

where z is the cosmological redshift. [19] However, because only a fraction of the energy is being filtered into the galactic medium, we need to add an efficiency factor [19] $f(z, m_\chi)$ to the equation:

$$\frac{dE}{dV\,dt} = f(z, m_\chi)\cdot(1+z)^6(\rho_c)^2\frac{\langle\sigma v\rangle}{m_\chi}.$$

We note that $f(z, m_\chi)$ is currently being bound by the Planck Telescope.

Of course, we will only have a definitive answer as to the energy rate equation only after the DM annihilation is finalized, but this provides an intriguing setup as to how we can utilize changes in the early ionization of the universe to configure DM. Currently, data from RECFAST, HyREC, and CosmoRec all provide methods to model how extra energy (like that from DM) yields different times of ionization, while the CLASS project illustrates methods to deal with the anisotropies. [19]

5.6 Decay

Many of the same principles of annihilation DM applies for decay. For example, the J-factor for annihilation can be easily transferred into the D-factor -

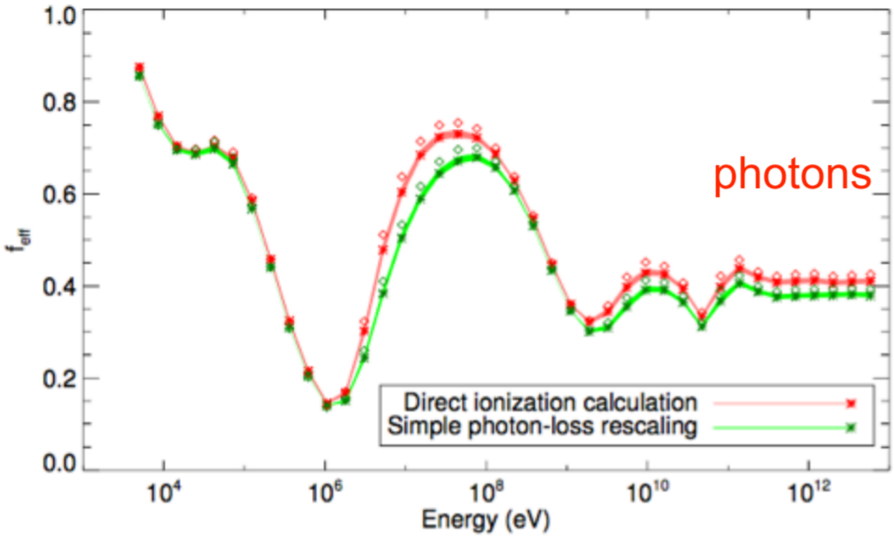

Figure 9: A depiction of the varying efficiency factors of energy ejections into the Inter-Galactic Medium; the exact mechanism for the curvature has yet to be discovered. Figure from [19].

$$D = \int \int \rho(l, \Omega) dl d\Omega,$$

and thus the flux equation remains the same except for the change in the exponent. [1] Here are some approximate D-factors from various dwarf galaxy sources, chosen for their low baryonic matter count. [15]:

Name	Distance[kpc]	$\theta_{\max}$	$\log_{10} D(\theta_{\max})[\text{GeV}^2\text{cm}^{-5}]$	$\log_{10} D(0.5°)[\text{GeV}^2\text{cm}^{-5}]$
Sextans	86 $\pm$4	1.7	$18.76^{+0.15}_{-0.15}$	$18.07^{+0.29}_{-0.29}$
Ursa Major	76 $\pm$3	1.37	$18.84^{+0.12}_{-0.12}$	$18.45^{+0.24}_{-0.24}$
Boötes	66 $\pm$2	0.47	$17.25^{+0.32}_{-0.19}$	$17.28^{+0.64}_{-0.38}$
Reticulum II	30 $\pm$3	1.0	$18.19^{+0.42}_{-0.17}$	$17.93^{+0.85}_{-0.32}$

The rate of decay is proportional to $e^{-\frac{t}{\tau}}$, while the rate at which energy is injected into the interglactic medium(IGM) can be expressed as

$$\frac{dE}{dVdt} = f(z, m_\chi) \cdot \frac{1}{\tau} \rho_c (1+z)^3,$$

where τ represents the lifetime constant of the dark matter particle. [19] This lifetime constant can be approximated utilizing a calculation similar to what is mentioned in the previous section. If τ were smaller than it actually is, then the influx of energy into the IGM would be much larger, affecting the CMB significantly and causing it to be at a higher energy state from what we see today. Clearly, this presents a fruitful route of research, as the CMB can help us get a tighter bound on τ if we can nail down $f(z, m_\chi)$, utilizing further mathematical models, and ρ_c by refining NFW profiles. [15]

In addition, due to the increase of research into the energy released from DM annihilation and decay affecting the ionization of the universe, physicists strongly postulate that the overall effects of DM on the reionization of the universe around $z = 6$ to $z = 10$. [19]

6 Current Research and Possible Future Experiments

We now discuss current research efforts in the realm of DM indirect detection that serve to pin down experimental values to yield a more precise estimate of DM density, annihilation rates, and cross sections. Despite a plethora of research, the entirety of gamma photons, neutrinos, and other particles detected come solely from the background that we expect.

6.1 Positron Emission

In addition to the gamma-ray and neutrino detection methods produced by DM annihilation, there are also other annihilation processes that create more SM routes. In particular, the AMS experiment aims to find positrons from DM annihilation - it produced a graph in 2016 that conveys a spike in observed positron flux versus the expected flux. [4]

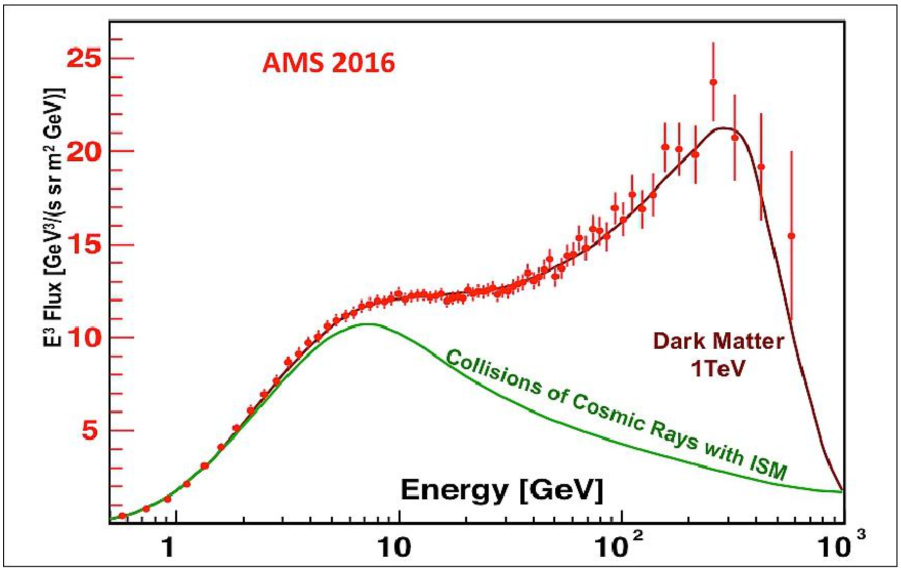

Figure 10: This is a graph of the positron flux observed by the Alpha Magnetic Spectrometer (AMS). The spike in positron flux is much larger that what we expected from the known astrophysical phenomena. While this spike could be caused by some astrophysical object, it is unlikely; rather, when we apply a DM model with a 1 TeV mass, the model best fits the spike (black line). Figure from [24]

This discrepancy can be explained when we look at the positron spectrum measurement made with the AMS experiment, CAPRICE, BESS, AMS, and PAMELA experiments along with our known measurements from secondary productions (interactions with baryonic matter). [4] When creating a comparison, a large portion of the positron spectrum seems to come from these secondary sources, but yet still a major component stems from sources unexplained by DM. However, the AMS 2016 experiment yielded fruitful results once they adjusted the DM energy as shown in Figure 9 - this could imply that DM could potentially be behind the creation of excess positrons. [24]

6.2 Cross Section Precision

We present some graphs of cross-section precision calculations of $\chi\chi \to \gamma\gamma$ and $\chi\chi \to e^+e^-$.

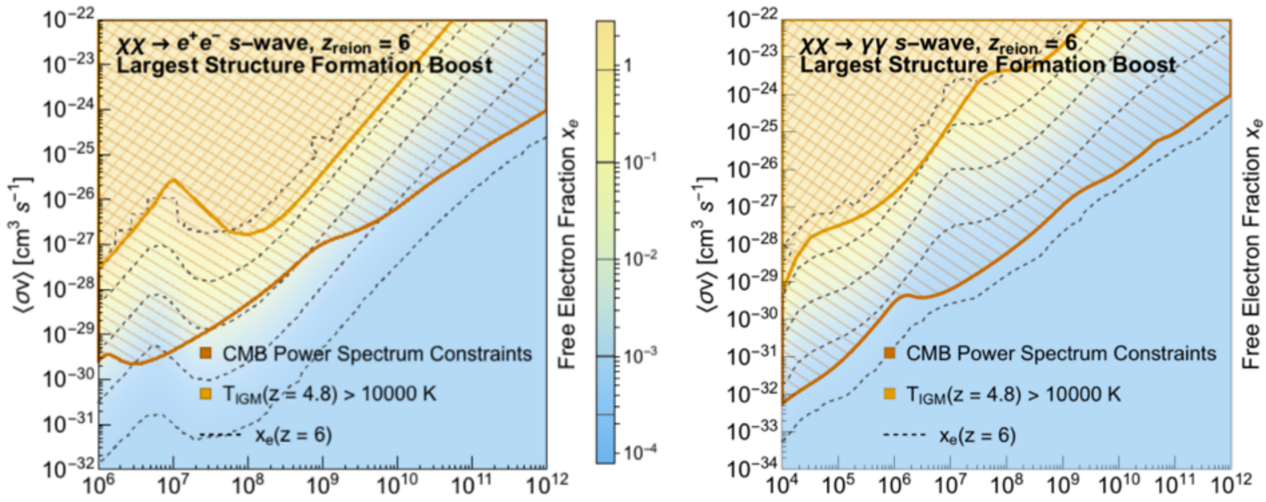

Figure 11: The graphs depicts both thermal and CMB bounds on DM for varying masses for both γ annihilation and e^+e^- annihilation. Figure from [19]

As discussed above, the amount of energy injected from DM annihilation is relatively large compared to background thermal energy, so it leaves an imprint on the CMB, which turns out to be a relatively fixed quantity. As a result, the tightest upper bound on the annihilation WIMP cross section comes from the CMB and is

$$\langle\sigma v\rangle_{CMB} \leq 4 \times 10^{-28}\,\frac{m_\chi}{f}\mathrm{cm}^3\mathrm{s}^{-1}.[25]$$

Moreover, the CMB further allows us to set a lower bound on the mass of the DM particle, as being 50 GeV if the WIMP is its own antiparticle and 100 GeV if the WIMP and its antiparticle differ. [25]

6.3 Supernovae to solve Core vs Cusp Problem

As discussed previously, the core v.s. cusp problem is a central puzzle in CDM density distributions as scientists attempts to see how changes in the gravitational landscape of a given galaxy propel fluctuations in the DM density, especially towards the centers of galaxies. In particular, the centers of galaxies are currently observed to have very flat curves for DM density, but after a certain radial distance, the density declines at a very steep power law - the adjoining point at which these different functions intersect is known as the "cusp." [1] The solution to this problem currently involves essentially "shaking-up" the gravity of the system. Even though after a supernova the majority of the gas expelled slows down due to radiation cooling and then returns to the center, the repetition of this process - which is currently being run within N-body simulations

- can cause the gravity of a galaxy to change fundamentally, thus modifying the DM density distribution as well. [12]

Currently, through this oscillatory technique, certain hydrodynamic simulations have developed sequences where the cusp is able to flatten out into a more continuous distribution - this depends strongly on the energy/expulsion of the supernovae, of course, but also the amount of time the expansions take. In particular, many models have utilized harmonic oscillations in order to model increasing and decreasing concentrations of gas. However, due to the differences between gravity and this setup, recent results have employed Fourier Analysis in order to pin the gas down. [12]

The different resonance states within models such as those of Ogiya and Mori suggest that when the period of oscillation is equivalent to to the local dynamic time that the core to cusp transition will occur within the galactic system. [12]

6.4 Collider Limits

In this section, we will discuss collider limits as a source of DM detection in which we search for discrepancies in observed and actual particle momenta. Due to conservation of momentum and the precise measurements of colliders, we hope to deduce that any missing momentum can either be a new particle or a DM particle. We set bounds on this missing energy for convenience during our search. For indirect detection, we consider all decay paths that stem from SM particles and look at the decay process to see if there is any missing momentum. [34]

In the case of Higgs decay indirect detection methods take into account all the possible branches for this decay and consider the percentage that will become DM neutralino pairs, a likely candidate for DM that comes from the Supersymmetry (SUSY) model. These are called branch fractions, which represent the percentage of particles that branch out in a certain pair, which in this case is the neutralino pair that we can infer is DM. The invisible branching fractions for $H \longrightarrow \chi\chi$, where H is a Higgs boson and χ is a neutralino, have upper bounds of 25 percent in the ATLAS experiment and 24 percent in the CMS experiment. [34] With this knowledge of the branching factors for Higgs decay, we can indirectly detect two DM particles being produced from our observed SM particle decay.

To observe DM in a particle collision, we search for two proton streams that interact and do not produce their intended products. In order for us to confirm the creation of DM, we look for a quark or gluon to be radiated off of the proton stream to tag the DM. Ultimately, we can set limits on specific energy losses, so we only must look in that range that produces DM particles.

7 Conclusion

7.1 Axions

The axion refers to a particle that was created to solve the polarity problem in the neutron. Within the neutron, the two down quarks and one up quark, their charges being $-\frac{1}{3}, -\frac{1}{3}$, and $+\frac{2}{3}$, are separated from each other at certain lengths, yielding the neutral particle that we observe. Due to the distinct charges within the neutron, we would expect a high polarity value (Debye scale) - however, the value that is actually observed is 1.4×10^{-16}, which is drastically smaller than expected. The incorporation of the axion attempts to explain the observed polarity. Its slow, inert, and stable characteristics make it compatible for many of the observed instances of DM in the universe, within halos in galaxies and clusters. The axion, if it is to be considered a DM particle, should not take part in chemical reactions, it must not decay (or must decay after a time longer than the age of the universe), and it must be relatively slow-moving and non-relativistic - and it satisfies all of these constraints. [3] Experiments such as the IAXO at CERN are attempting to find it through its conversion into a photon through interactions with electromagnetic fields. This is yet another method used to prove the existence of DM and can prove fruitful with time. Much of the research is devoted to exacting the mass range of the axion and calculating whether it is compatible with other DM predictions. [3]

7.2 Direct Detection

The direct detection of DM is another form of DM detection that strives to collect signals from an individual DM particle, instead of measuring end-products of annihilation and decay reactions. Typically measuring from the Milky Way's DM halo, researchers are creating state-of-the-art detectors to observe an individual WIMP particle scatter off an atomic nuclei. A specific example is the Large Underground Xenon Experiment (LUX), which aims to find the photons produced from the scattering of DM particles. [26] The use of Xenon - which has a relatively high nucleus - provides a greater cross section for the DM to hit, meaning the LUX will be more likely to detect DM since it uses a large volume of large cross section particles. By finding the proportionality of the amount of light detected compared to the energy dissipated, LUX will be able to detect these DM particle. More technically, DM direct detection theorists attempt to model the velocity distribution of individual WIMP particles, thus allowing them to compute WIMP energies; in the event of a collision, they postulate the recoil energies of DM colliding with a given nuclei and attempt to discern a distinctive signal. [26] Simple models attempt to pin down the velocity distribution as Gaussian or Maxwell-Boltzman:

$$f(v)dv = \frac{vdv}{v_e v_0 \sqrt{\pi}} \left(\exp\left(-\frac{(v-v_e)^2}{v_0^2} \right) - \exp\left(-\frac{(v+v_e)^2}{v_0^2} \right) \right),$$

where $v_0 = 220 \text{ km s}^{-1}$ and v_e are the velocity of the sun around the center of the galaxy and the earth around the sun, respectively. [26] From such models, the total flux of DM within a local region can be computed - with much room for error, of course. As a result, efforts look towards pinning down the correct form for $f(v)$ and the recoil energy E_R:

$$E_R = \frac{\mu^2 v^2}{m_N}(1 - \cos\theta).[26]$$

Here, m_N is the mass of the scattering nucleus, q is a momentum transfer quantity, θ is the scattering angle, and μ is the reduced mass.

Current research also is attempting to refine this model and reduce error wherever possible.

7.3 Modified Gravity

Modified gravity is an attempt to explain rotation curves by modifying Newtonian Mechanics. It claims that DM is actually nonexistent and that the observed astronomical phenomena are a result of an unknown form of modified gravity. In the case of rotation curves, modified gravity claims that we have not yet measured acceleration that slow yet [2]. The theory states that the Newtonian equation $F = ma$, is can be rewritten as:

$$F = ma\mu\left(\frac{a}{a_0}\right),$$

where μ is a speculative "interpolation" function of acceleration with no definitive form. [16] The theory claims that when the ratio of $\mu(\frac{a}{a_0}) \gg 1$ that μ is equal to one, reducing to Classical

Mechanics. However, when $\mu(\frac{a}{a_0}) \ll 1$, then the function will equal $\frac{a}{a_0}$, making Newton's 2nd Law

$$F = \frac{ma^2}{a_0},$$

which confirms our analysis of rotational curves. [16] The use of modified gravity, nevertheless, fails to explain as many phenomena as DM particles would and the cause of the peaks in CMB resonance graphs. Where we can easily explain these phenomena through cold DM interacting with the baryonic matter, modified gravity cannot. [4] It is not a very popular theory for the explanation of DM, but it is still plausible.

References

[1] Lisanti, M. (2016). Lectures on Dark Matter Physics. https://doi.org/10.1142/9789813149441$_0$007

[2] Mariangela Lisanti - Particle Phenomenology for String Theorists 1 - YouTube. (n.d.). Retrieved July 27, 2018, from https://www.youtube.com/watch?v=STXZWyzlgxMt=3154s

[3] Jesse Thaler, MIT, quot;Confronting the Invisible Universequot; - YouTube. (n.d.). Retrieved July 27, 2018, from https://www.youtube.com/watch?v=QNmSNY8VenQ

[4] Bertone, G., Hooper, D. (2016). A History of Dark Matter. Retrieved from http://arxiv.org/abs/1605.04909

[5] Slatyer, T. R. (n.d.). TASI Lectures on Indirect Detection of Dark Matter. Retrieved from http://www.ams02.org/

[6] Wilson, R. W. (1979). The cosmic microwave background radiation. https://doi.org/10.1126/science.205.4409.866

[7] Waynehu. (n.d.). Retrieved July 31, 2018, from http://background.uchicago.edu/ whu/power/bao.html

[8] Pires, S. (2009). Light on Dark Matter with Weak Gravitational Lensing. Retrieved July 31, 2018, from https://arxiv.org/pdf/0908.4157.pdf

[9] Dark Matter and Galaxy Rotation - YouTube. (n.d.). Retrieved July 27, 2018, from https://www.youtube.com/watch?v=fUAzc1evIBo

[10] Gaskins, J. M. (2016). A review of indirect searches for particle dark matter. Month, 00(00), 1–32. https://doi.org/10.1080/0010751YYxxxxxxxx

[11] Okoli, C. (n.d.). Dark matter halo concentrations: a short review. Retrieved from https://arxiv.org/pdf/1711.05277.pdf

[12] Ogiya, G., Mori, M. (2010). The core-cusp problem in Cold Dark Matter halos and supernova feedback. AIP Conference Proceedings, 1279(12pp), 403–405. https://doi.org/10.1063/1.3509326

[13] Villa-Vargas, J., I., Heller, C. (2010, July 28). Dark Matter Halos and Evolution of Bars in Disk Galaxies: Varying Gas Fraction and Gas Spatial Resolution. Retrieved July 31, 2018, from https://arxiv.org/abs/1004.4899

[14] Danninger, M. (2017). Review of indirect detection of dark matter with neutrinos. Journal of Physics: Conference Series, 888(1), 12039. https://doi.org/10.1088/1742-6596/888/1/012039

[15] Evans, N. W., Sanders, J. L., Geringer-Sameth, A. (n.d.). Simple J-Factors and D-Factors for Indirect Dark Matter Detection. Retrieved from https://arxiv.org/pdf/1604.05599.pdf

[16] Milgrom, M. (2015). MOND Theory. Retrieved July 31, 2018, from https://arxiv.org/pdf/1404.7661.pdf

[17] Physics | iaxo.web.cern.ch. (n.d.). Retrieved July 27, 2018, from http://iaxo.web.cern.ch/content/physics

[18] AMS-02 » Archive » The First Five Years of the Alpha Magnetic Spectrometer on the International Space Station. (n.d.). Retrieved July 27, 2018, from http://www.ams02.org/2016/12/the-first-five-years-of-the-alpha-magnetic-spectrometer-on-the-international-space-station/

[19] Slatyer, T. (n.d.). Constraints on Dark Matter from the Cosmic Microwave Background. Retrieved July 31, 2018, from https://indico.fnal.gov/event/13702/session/5/contribution/7/material/slides/0.pdf

[20] Vincent, A. (n.d.). (11) Constraining Annihilating Dark Matter with the Cosmic Microwave Background - YouTube. Retrieved July 29, 2018, from https://www.youtube.com/watch?v=Cy3yX9U$_{oU}$

[21] Rowell, G. (n.d.). Dark matter searches with gamma-rays (HESS-II, CTA, Fermi-LAT) CAASTRO-CoEPP Workshop (Great Western) Sept. 2014. Retrieved from https://indico.cern.ch/event/338929/attachments/664193/913005/Gavin$_{R}owell.pdf$

[22] Goodenough, L., Hooper, D. (2009). Possible Evidence For Dark Matter Annihilation In The Inner Milky Way From The Fermi Gamma Ray Space Telescope. Retrieved from https://arxiv.org/pdf/0910.2998.pdf

[23] A History of Dark Matter- Gianfranco Bertone amp; Dan Hooper. (n.d.). Retrieved July 31, 2018, from https://ned.ipac.caltech.edu/level5/Sept16/Bertone/Bertone4.html

[24] American Mathematical Society. (n.d.). Retrieved from http://www.ams.org/publicoutreach/feature-column/fcarc-grav$_{l}ens$

[25] Steigman, G. (2015). CMB Constraints On The Thermal WIMP Mass And Annihilation Cross Section. Retrieved July 31, 2018, from https://arxiv.org/pdf/1502.01884.pdf

[26] Klasen, M. (2015). Indirect and direct search for dark matter. Retrieved July 31, 2018, from https://arxiv.org/pdf/1507.03800.pdf

[27] CMB Angular Spectrum Graph. (n.d.). Retrieved July 31, 2018, from https://map.gsfc.nasa.gov/media/080999/index.html

[28] Ogiya, G., Burkert, A. (2015). Re-examining the too-big-to-fail problem for dark matter haloes with central density cores. Monthly Notices of the Royal Astronomical Society, 446(3), 2363–2369. https://doi.org/10.1093/mnras/stu2283

[29] Charles, E. (2017). Indirect Dark Matter Searches: a Review. Retrieved from http://vietnam.in2p3.fr/2017/dm/transparencies/1$_{m}onday/1_{m}orning/4_{c}harles.pdf$

[30] Navarro, J. F., Frenk, C. S., White, S. D. M., Fellow, B. J. B. (1995). The Structure of Cold Dark Matter Halos. Retrieved from https://xxx.lanl.gov/pdf/astro-ph/9508025v1

[31] Rubinf, V. C., Ford, W. K. (1970). (c) 1970. The University of Chicago. All rights reserved. The Astrophysical Journal (Vol. 159). Retrieved from http://articles.adsabs.harvard.edu/cgi-bin/nph-iarticle$_{q}uery?1970ApJ...159..379Ramp; data_{t}ype = PDF_{H}IGHamp; whole_{p}aper = YESamp; type = PRINTERamp; filetype = .pdf$

[32] Science-in-progress: Did the Bullet Cluster withstand scrutiny? | Ars Technica. (n.d.). Retrieved August 3, 2018, from https://arstechnica.com/science/2017/09/science-in-progress-did-the-bullet-cluster-withstand-scrutiny/

[33] Mariangela Lisanti - Particle Phenomenology for String Theorists 3 - YouTube. (n.d.). Retrieved August 4, 2018, from https://www.youtube.com/watch?v=RFAkvmetOJIt=4482s

[34] EUROPEAN ORGANIZATION FOR NUCLEAR RESEARCH (CERN)-BY-3.0 license. (2017). https://doi.org/10.1007/JHEP02(2017)135

[35] Primer On WIMP Dark Matter. | The Eternal Universe. (n.d.). Retrieved August 9, 2018, from http://theeternaluniverse.blogspot.com/2009/12/primer-on-wimp-dark-matter.html